Galaxy Evolution and Feedback across Different Environments
Proceedings IAU Symposium No. 359, 2020
T. Storchi-Bergmann, W. Forman, R. Overzier & R. Riffel, eds.
doi:10.1017/S1743921320001568

From global to local scales in galaxies

Sebastian F. Sánchez and Carlos Lopez Cobá

Instituto de Astronomía, Universidad Nacional Autonóma de México,
A.P. 70-264, 04510 México, D.F., Mexico
email: sfsanchez@astro.unam.mx

Abstract. We summarize here some of the results reviewed recently by Sanchez (2020) comprising the advances in the comprehension of galaxies in the nearby universe based on integral field spectroscopic galaxy surveys. In particular we explore the bimodal distribution of galaxies in terms of the properties of their ionized gas, showing the connection between the star-formation (quenching) process with the presence (absence) of molecular gas and the star-formation efficiency. We show two galaxy examples that illustrates the well known fact that ionization in galaxies (and the processes that produce it), does not happen monolitically at galactic scales. This highlight the importance to explore the spectroscopic properties of galaxies and the evolutionary processes unveiled by them at different spatial scales, from sub-kpc to galaxy wide.

Keywords. galaxies: evolution, galaxies: star-formation, galaxies: ISM

1. Integrated properties of galaxies

Along the last years our knowledge of nearby galaxies ($z < 0.1$) and the comprehension of the evolutionary processes that have produced them have been considerably increased due to the advent of large and statistical significant imaging and spectroscopic galaxy surveys (e.g., Sloan Digital Sky Survey, SDSS, Galaxy and Mass Assembly survey, GAMA York *et al.* 2000; Driver *et al.* 2009). They have allowed us to explore the multi-band photometry and imaging of millions of galaxies, providing with single aperture spectroscopic observations of hundred of thousand of them. A recent review by Blanton & Moustakas (2009) have summarized the main results derived from these surveys, including their global distributions in colors, luminosities, stellar and atomic gas masses and fractions and their corresponding mass/luminosity functions, for different galaxy types and environments.

The comparison of the properties of galaxies at $z \sim 0$ explored by these surveys with those derived at different redshifts have demonstrated that all galaxies formed stars in the past, at a much higher rate than today (e.g. Heavens *et al.* 2004; Speagle *et al.* 2014; Madau & Dickinson 2014). However, in the last $\lesssim$8 Gyr galaxies present a clear bimodal distribution in terms of their star-formation activity, with two well distinguished populations: (i) disk-dominated, dynamically supported by rotation late-type galaxies, actively forming stars and (ii) bulge-dominated, with a large fraction of hot and warm stellar orbits, early-type galaxies, currently retired from the star-formation budget. These two groups are well separated in different diagrams, like the color-magnitude (or age-mass), or the SFR-M$_*$ (e.g. Renzini & Peng 2015), where the distinction is stronger than in any other one. This separation is evident when using the average EW(Hα), a parameter strongly correlated with the sSFR (i.e., $\frac{SFR}{M_*}$, the two parameters involved in the SFR-M$_*$ diagram). Retired galaxies (RGs) in general present low EW(Hα) (<3Å, Stasińska *et al.* 2008), exhibiting in the majority of the cases a weak emission of ionized gas, with line

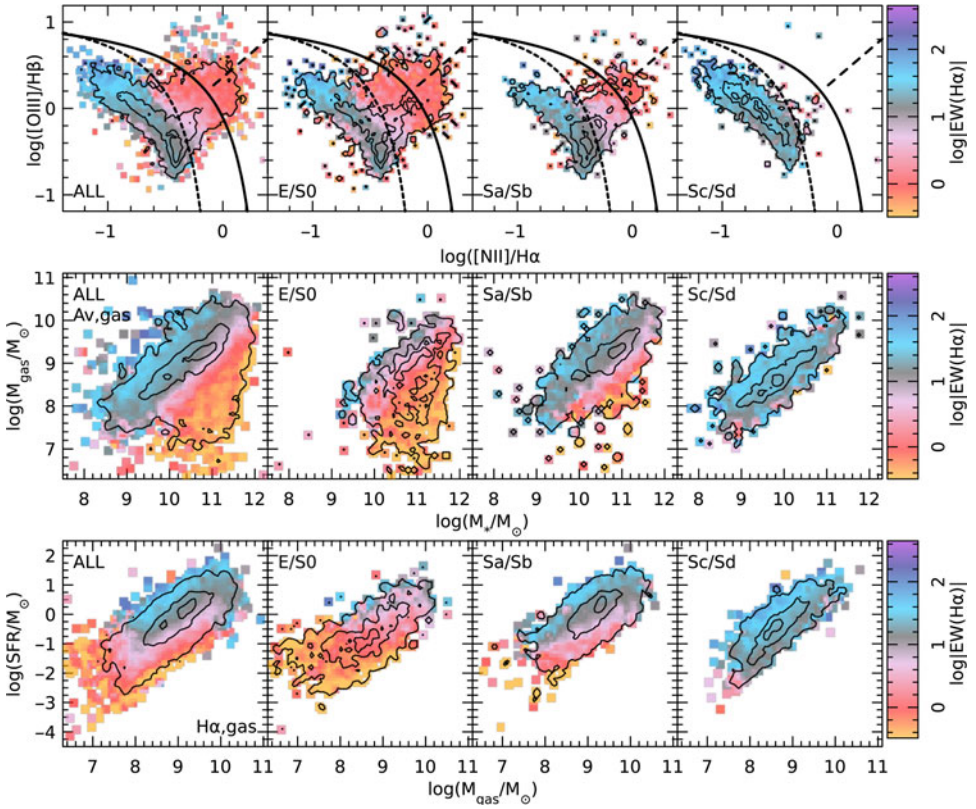

Figure 1. *Top panels:* BPT diagnostic diagram for the emission lines of the ionized gas observed in the considered sample of galaxies, averaged in a ring at one effective radius. The left-most panel show the distribution for all the galaxies, with similar distributions segregated by morphology shown in the subsequent panels, from earlier types to later ones from left to right. *Middle panels:* Distribution of the gas mass estimated from the dust attenuation derived by the Hα/Hβ line ratios, along the stellar masses of the galaxies in the same sample. *Bottom panels:* Similar figure showing the distribution of the integrated SFR derived from dust-corrected Hα luminosity along the gas mass estimated for each galaxy. Along all panels the density distributions are shown as successive contours including a 95%, 50% and 10% of the points, while the colormaps indicate the average logarithm of the EW(Hα) at a particular location.

ratios indicating the presence of a hard ionizing source. Star-forming galaxies (SFGs), present in general higher values of the EW(Hα) (>10Å Lacerda *et al.* 2018), with stronger ionized emission, and line ratios compatible with a softer ionizing source. On top of that, strong AGNs present strong emission lines, with large values of EW(Hα) (> 6Å, Cid Fernandes *et al.* 2010), and hard ionizing sources. In general, RGs are associated with early-type galaxies, while SFGs are dominated by late-type ones. Figure 1 illustrates this segregation, showing clear differences in the distribution of galaxies of different morphologies across the classical diagnostic diagrams (e.g. Baldwin *et al.* 1981, BPT diagram), and their average EW(Hα). For this particular diagram we use the compilation of optical integral field spectroscopic (IFS) data recently presented by Sanchez (2020), comprising more than 8000 galaxies observed by different IFS galaxy surveys in the nearby universe: CALIFA (Sánchez *et al.* 2012), MaNGA (Bundy *et al.* 2015), SAMI (Croom *et al.* 2012) and AMUSSING++ (López-Cobá *et al.* 2020). All data have been processed using the same pipeline, (Pipe3D Sánchez *et al.* 2016), in order to homogenize at maximum this heterogeneous compilation.

https://doi.org/10.1017/S1743921320001568 Published online by Cambridge University Press

The bimodal distribution in the different described diagrams indicates that the necessary transition between SFGs (all galaxies at very high-redshift), and the current observed population of RGs (which increases towards $z \sim 0$, e.g., Muzzin *et al.* 2013) should be rather fast (compared to the Hubble type, i.e., $\lesssim$1 Gyr, e.g., Sánchez *et al.* 2019). This transition involves a morphological transformation, and therefore should be somehow connected to the dynamical stage of galaxies (e.g. Martig *et al.* 2009). It may involve a highly and short-lived process that injects energy to the system heating or removing gas, i.e., the main ingredient of the SF process (an AGN?, e.g. Hopkins *et al.* 2009). The presence of AGN hosts in the transition regime (Green-Valley) between the SFGs and RGs in different diagrams seems to support this hypothesis (e.g. Schawinski *et al.* 2014; Sánchez *et al.* 2018). Whatever is the triggering mechanism of the quenching, what it is clear is that RGs present a general deficit of cold gas (molecular gas in particular, Saintonge *et al.* 2016; Sánchez *et al.* 2018). This is clearly observed in the distribution of integrated gas mass (M_{gas}) along the stellar mass (M_*) seen in Fig. 1, middle panel. Indeed, lack of (molecular) gas, either removed or heated, seems to be the primary driver (or connection) with the observed decrease of SF in quenched/RGs. Actually, the segregation is stronger regarding the amount of (molecular) gas, than regarding the efficiency in how this gas is transformed to stars (defined as SFE= $\frac{SFR}{M_{gas}}$). Fig. 1, bottom panel, shows the integrated SFR along M_{gas}, i.e., the integrated version of the Schmidt-Kennicutt law (Kennicutt 1998), segregated by morphology, and highlighted by the EW(Hα). Retired or partially retired galaxies form stars at a slightly lower rate than SF ones for the same amount of (molecular) gas. However, they present a much lower amount of SFR because they have a much lower amount of gas. Among SFGs, SFE and gas fraction seems to equally compete to explain the distribution along the main trends (e.g., Sa/Sb galaxies).

2. Local processes in galaxies

Despite of the tremendous improvement in our understanding of galaxies provided by the quoted surveys, they still provide with an incomplete picture of the evolution processes in galaxies. While the information provided by imaging survey allow us to explore the spatial resolved distribution of light, stellar mass, and the morphological properties of galaxies, the spectroscopic information is in general limited to a single aperture that, in many cases, samples different physical extensions of the objects depending on their redshift (and in most cases biased towards their central regions). In general, the studies based on these surveys consider galaxies as unresolved entities, being either SF or retired, and assuming that any process happens simultaneously across their full extension. Therefore, they cannot provide with a real description of processes that occur at kpc or sub-kpc scales.

For instance, the condensation of diffuse atomic gas into molecular clouds, and the dynamical collapse of that clouds to give birth to stars are not processes that happen at a galactic scale. This is evident when exploring the distribution of recently formed young stars in galaxies, traced by the H II regions. Figure 2, top panel, shows both a three-color continuum image (u-, g- and r-band) and an emission line image ([O III], Hα and [N II]), of the late-type galaxy 2MASXJ09534925+0911377. This latter image is mapped into a spatial resolved BPT diagnostic diagram. The central/bulge dominated regions of the galaxy present by a weak, diffuse, hard ionization that exhibits low values of the EW(Hα), located at the right-hand side of the BPT diagram (in the LINER-like regime). This ionization is produced by either hot-evolved/post-AGB stars (e.g. Binette *et al.* 1994; Singh *et al.* 2013) or slow velocity shocks (e.g. Dopita *et al.* 1996). On the contrary, the disk of this galaxy presents a series of clumpy ionized regions with strong, but softer ionization, that have large values of the EW(Hα), located in the BPT diagram at the

https://doi.org/10.1017/S1743921320001568 Published online by Cambridge University Press

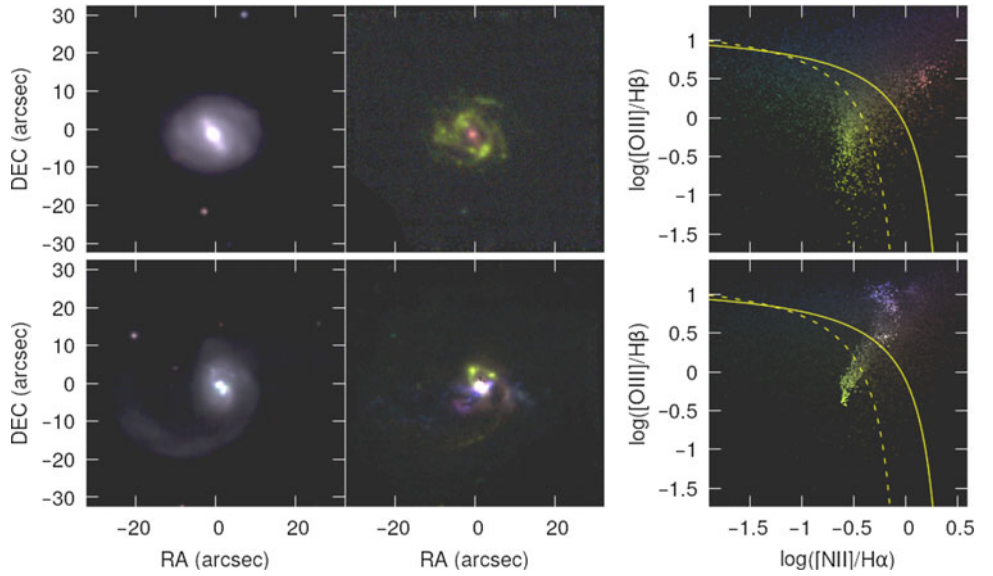

Figure 2. *Left panels:* Three-color continuum images created using g (blue),r (green) and i-band (red) images extracted from the MUSE datacube of 2MASXJ09534925+0911377 (top panels) and ESO253-G003 (bottom panels) galaxies,. *Middle panels:* Emission line image created using the [O III] (blue), Hα (green) and [N II] (red) emission line maps extracted from the same datacube using PIPE3D. *Right panels:* Spatial resolved classical BPT diagnostic diagram involving the [O III]/Hβ and [N II]/Hα line ratios, color-coded by the values in the emission line image shown in the middle panel for each spaxel. The solid- and dashed-lines represent the location of the Kewley *et al.* (2001) and Kauffmann *et al.* (2003) demarcation lines, respectively.

classical location of H II regions (e.g., Osterbrock 1989). Those are the signatures of star-forming regions (e.g. Espinosa-Ponce *et al.* 2020). Thus, this figure illustrates that neither star-formation (located in clumpy regions across the disk), not quenching (evident in the central regions), happens simultaneously through the optical extension of galaxies. This is also true for any other ionization process observed in galaxies. Fig. 2, bottom panel, shows similar plots for the galaxy merger ESO253-G003. Like in the previous case, this galaxy presents strong star-forming regions, seen as green nodules in the emission line combined image, in particular two gigantic ones at the north of the two cores of the merging galaxies. However, contrary to the previous case, this galaxy has a strong, hard ionization and well peaked emission in the central regions, with high values of the EW(Hα). This is the clear signature of an AGN (Cid Fernandes *et al.* 2010; Gomes *et al.* 2016). On top of that, the hard ionization is distributed along a set of filamentary/clumpy structures emanating from the the central regions and distributed following a more or less biconical structure at both the east and west side of the interacting galaxies. Those are clear signatures of galactic scale outflows (e.g. López-Cobá *et al.* 2020). Therefore, it is evident that the physical processes that produce the ionization in galaxies, that are related with the evolutionary processes in galaxies (star-formation, retirement, AGN activity, outflows, quenching...), does not happens monolitically and simustaneously at a galactic scale. Despite that this is a rather simple, evident and accepted known fact, all these processes have been widely explored and explained as if this was not the case.

The advent of wide-field and multiplexed Integral Field Units (IFUs) in the last decade has allowed to adopt a completely different approach in the exploration of galaxies (in general), and those better resolved (i.e., the ones at the nearby universe). The application of this technique over large and well defined statistical samples of galaxies have allowed us

https://doi.org/10.1017/S1743921320001568 Published online by Cambridge University Press

to uncover local/spatial resolved relations and patterns. Among them, the most relevant ones show that: (i) ionization processes in galaxies happen at local scales, and can be understood only by the combined exploration of line-ratios, EW(Hα), morphology/shape of the ionized structures and kinematic analysis (e.g., Fig. 2 López-Cobá *et al.* 2020); (ii) the global scaling relations observed among SFGs, like the SFMS, the Mgas-M$_*$, the SK-law or the Mass-Metallicity relation, have local counter-parts that indeed explain both the global ones and the radial gradients observed in many properties across the optical extension of galaxies; (iii) galaxies seem to grow from the inside-out, at least those more massive than $10^{9.5}$M$\odot$, presenting a local/resolved downsizing, meaning that more massive regions (in terms of Σ_*) in galaxies evolves faster than less massive ones; (iv) finally, quenching happens too from the inside-out, strongly connected with bulge growth (and thus, with the presence of hot orbits). The results of all these recent IFS-GS have been reviewed recently in Sanchez (2020), including a detailed explanation of the data used along this manuscript.

References

Baldwin, J. A., Phillips, M. M., & Terlevich, R. 1981, *PASP*, 93, 5
Binette, L., Magris, C. G., Stasińska, G., & Bruzual, A. G. 1994, *A&A*, 292, 13
Blanton, M. R. & Moustakas, J. 2009, *ARA&A*, 47, 159
Bundy, K. Bershady, M. A., Law, D. R., *et al.* 2015, *ApJ*, 798, 7
Cid Fernandes, R., Stasińska, G., Schlickmann, M. S., *et al.* 2010, *MNRAS*, 403, 1036
Croom, S. M., Lawrence, J. S., Bland-Hawthorn, J., *et al.* 2012, *MNRAS*, 421, 872
Dopita, M. A., Koratkar, A. P., Evans, I. N., *et al.* 1996, in Astronomical Society of the Pacific Conference Series, Vol. 103, The Physics of Liners in View of Recent Observations, ed. M. Eracleous, A. Koratkar, C. Leitherer, & L. Ho, 44
Driver, S. P., Norberg, P., Baldry, I. K., *et al.* 2009, *Astronomy and Geophysics*, 50, 5.12
Espinosa-Ponce, C., Sánchez, S. F., Morisset, C., *et al.* 2020, *MNRAS*, 494, 1622
Gomes, J. M., Papaderos, P., Vílchez, J. M., *et al.* 2016, *A&A*, 585, A92
Heavens, A., Panter, B., Jimenez, R., *et al.* 2004, *Nature*, 428, 625
Hopkins, P. F., Cox, T. J., Younger, J. D., *et al.* 2009, *ApJ*, 691, 1168
Kauffmann, G., Heckman, T. M., Tremonti, C., *et al.* 2003, *MNRAS*, 346, 1055
Kennicutt, Jr., R. C. 1998, *ApJ*, 498, 541
Kewley, L. J., Dopita, M. A., Sutherland, R. S., *et al.* 2001, *ApJ*, 556, 121
Lacerda, E. A. D., Cid Fernandes, R., Couto, G. S., *et al.* 2018, *MNRAS*, 474, 3727
López-Cobá, C., Sánchez, S. F., Anderson, J. P., *et al.* 2020, *AJ*, 159, 167
Madau, P., & Dickinson, M. 2014, *ARA&A*, 52, 415
Martig, M., Bournaud, F., Teyssier, R., *et al.* 2009, *ApJ*, 707, 250
Muzzin, A., Marchesini, D., Stefanon, M., *et al.* 2013, *ApJ*, 777, 18
Osterbrock, D. E. 1989, Astrophysics of gaseous nebulae and active galactic nuclei (University Science Books)
Renzini, A., & Peng, Y.-j. 2015, *ApJL*, 801, L29
Saintonge, A., Catinella, B., Cortese, L., *et al.* 2016, *MNRAS*, 462, 1749
Sanchez, S. F. 2020, *ARA&A*, 58, 99
Sánchez, S. F., Kennicutt, R. C., Gil de Paz, A., *et al.* 2012, *A&A*, 538, A8
Sánchez, S. F., Pérez, E., Sánchez-Blázquez, P., *et al.* 2016, *Rev. Mexicana Astron. Astrofis.*, 52, 171
Sánchez, S. F., Avila-Reese, V., Hernandez-Toledo, H., *et al.* 2018, *Rev. Mexicana Astron. Astrofis.*, 54, 217
Sánchez, S. F., Avila-Reese, V., Rodríguez-Puebla, A., *et al.* 2019, *MNRAS*, 482, 1557
Schawinski, K., Urry, C. M., Simmons, B. D., *et al.* 2014, *MNRAS*, 440, 889
Singh, R., van de Ven, G., Jahnke, K., *et al.* 2013, *A&A*, 558, A43
Speagle, J. S., Steinhardt, C. L., Capak, P. L., *et al.* 2014, *ApJS*, 214, 15
Stasińska, G., Vale Asari, N., Cid Fernandes, R., *et al.* 2008, *MNRAS*, 391, L29
York, D. G., Adelman, J., Anderson, Jr., J. E., *et al.* 2000, *AJ*, 120, 1579

https://doi.org/10.1017/S1743921320001568 Published online by Cambridge University Press